

# ESTIMATION OF ENERGY RELEASE IN PROTON-21 EXPERIMENTS

A. Paschenko, V. Petukhov, I. Shapoval

For more than one decade, the Proton-21 Electrodynamics Laboratory staff executed a lot of successful experiments (above 20,000) and theoretical studies concerning the realization of the self-organizing nuclear fusion as an ecologically safe source of energy. The significant part of the results of scientific-research studies is presented in book [1] published by Springer-Verlag in 2007 and was reported on a number of international conferences.

However, some results related to the estimation of the energy released in the course of the synthesis were not sufficiently clarified. In what follows, we will give a brief survey of the results of modeling and evaluation of the positive energy gain in the Setup constructed at the Proton-21 Laboratory.

In order to determine the value of positive energy gain and the efficiency coefficient (denoted by  $\mathcal{Q}$ ), we need the comprehensive analysis of the energy balance in the Setup. Given the contribution of the energy of a primary driver to a target – anode, we need the diagnostics of the energy released at the target explosion. In this case, all possible channels of the energy release should be very carefully considered to exclude the errors. However, such an approach is associated with the necessity to use a high-cost measuring equipment and high-tech methods of its application. Therefore, the preliminary choice and the tough planning of efficient direct measurements with minimization of expenses are required. The orientational estimates presented in this work serve to the optimization of such a way, not replacing the necessity of direct measurements.

Since the consecutive account for channels of the energy release is additive, the positive energy balance due to the energy release already on a part of elements of the construction of the chamber of a diode and for a part of the main processes running in the Setup will ensure the positive energy balance on the Setup on the whole.

Here, we consider the mechanical deformations of a polyvinyl chloride tube (PVCT), which were directly observed in a large series of experiments and are sufficiently clear for the analysis of the process of energy release. PVCT is a structural functional part of the cathodic system (Fig. 1). It is a cylinder with axial cavity. Its internal surface has a spiral-like relief. As a result of the basic processes running in the Setup, the deformations of PVCT attract our attention by that the mentioned spiral-like relief turns out outside of the deformed tube. In other words, PVCT was inverted inside out. We were faced with the question about the space-time character and the energy of the action on the PVCT surface, which resulted in the final topological shape of a tube observed in experiments. It is clear that this transformation of PVCT occurs due to a time-dependent pressure of explosion products on its surface.

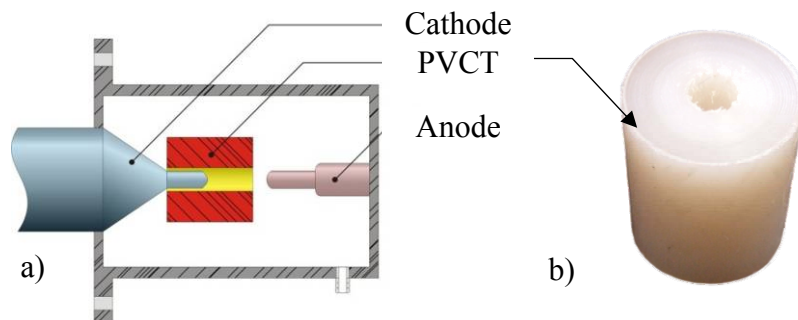


Fig. 1. Position of PVCT in the unit of the Setup (a) and the photo of PVCT in the initial state (b)

The direct experimental determination of the released energy meets certain difficulties. Therefore, the application of the method of simulation to the evaluation of the above-mentioned process seems to be suitable. We decided to use the experimental data accumulated at the Laboratory on magnitudes and kinds of deformation for the determination of the model adequacy degree and the validity of estimates of the energy release in the Setup.

In the simulation, we use the finite element method allowing us, on the one hand, to completely and conveniently parametrize the object under study and, on the other hand, to realize the arbitrarily detailed development of a deformation of PVCT in a series of model experiments [2, 3].

These numerical experiments were aimed at the attainment of a final strained state by a tube under experimental conditions on the Setup and at the determination of the energy required for a specific shape and a degree of deformation. The model must adequately describe the main properties of the processes, and its consequences should be transparent for the interpretation.

The main estimates were obtained within the proposed model of PVCT in the approximation of the *elasticity* of the processes of its shape-forming in the frame of the mechanics of deformed solids. It is known [8] that the behavior of a material under dynamical loads of the object depends essentially on the load application rate, loading history, load amplitude, force action duration, etc. Under different conditions of the action on a material, such properties as viscoplasticity, viscoelasticity, creep, and elasticity can be revealed. At high loading rates and the force amplitudes not causing the brittle or viscous fracture, the polymers are characterized by elastic deformations induced by not only by mutual displacements of atoms, but also by the motion of separate parts of macromolecules [8]. The mechanisms of plasticity of polymers are manifested at sufficiently large durations of the action (seconds and more). At a force load acting during several microseconds and at sufficiently large amplitudes, the strength of a material can increase, and, respectively, the energy required for a change of its shape increases as well. It is asserted [9, 10] that a polymer even in the liquid state under the application of a short-time load can reveal the properties of a solid and can demonstrate a high strength.

In view of the duration of the electromagnetic processes running in the Setup before the explosion and the measured time of action of the flows of a substance from the “hot dot,” the force acts on PVCT for **several microseconds**, i.e., the load is short-time. This is also indicated by the experimental measurements of voltages, currents, flows of particles, and temperature fields [1]. Thus, these facts testify in the favor of the elasticity-based model, in which the plasticity-involved processes have no time to occur. In addition, the simulation of elastic properties within the method of finite elements coincides in many cases with that of plastic properties, which supports the use of the elasticity-based model.

Some part of tubes deformed by explosions conserved their integrity. Just in these cases, the modeling of changes in the shape of PVCT gave the estimate of the minimum energy released on PVCT relative to that in the cases with the rupture of PVCT. The behavior of finite elements under loads of the order of 11 GPa indicates that we approach the threshold of the viscous or brittle fracture. In view of this fact, we established the interval of loads for estimations within the elasticity-based model.

We considered a possible mechanism of deformation of PVCT on the basis of the forces of electrostatic repulsion of surfaces bearing charges of the same sign and showed that such a scenario did not lead to the observed final states of a strained PVCT.

The flows of a substance acting on the tube were modeled by setting the pressures on the surfaces of the tube that underwent this action in correspondence with the location of PVCT in the Setup (Fig. 1). These pressures depended on the time and formed the field of pressure-induced forces modeled in computer-based experiments. At the modeling, the pressure amplitudes took values from several tens of MPa to 10 GPa, and the force action duration varied from several tens of nanoseconds to several microseconds.

In these intervals, we have realized the simulation of changes of the PVCT shape observed in experiments.

In the presence of significant deviations from the averaged force configurations shown in Figs. 2 and 3, the results of modeling did not correspond to the experimental ones, since one or other type of deformation was not realized due to the smallness of the duration or amplitudes of the force action, or the behavior of the pattern obtained within the method of finite elements at high loads indicated the fracture of the tube. We omitted such results of modeling. Therefore, we state that the space-time distribution of loads on the tube (Figs. 2 and 3) is unique to a certain extent, because the

introduction of a deviation from it into the modeling procedure led always to results sharply different from experimentally observed strained states of PVCT.

By modeling, we have studied the **whole collection** of experimentally observed final states of PVCT, being a deformed element of the Setup. This collection is diverse to a significant extent, is “dense,” and describes the sequence of various phases of deformations observed in experiments:

- Halved inversion of a monolithic tube;
- Full inversion of a monolithic tube without the creeping on the rod-holder (the cone, whose base is conjugated with the cylinder) positioned behind the tube;
- Full inversion of a monolithic tube with its creeping on the rod-holder;
- Inversion of a tube with its creeping on the rod-holder up to the stage of fracture of the tube;
- Deformations of a two-layer tube.

The comparison of the series of experimentally observed and simulated final states of PVCT given in Table 1 testifies to a good visual coincidence of shapes. This fact indicates that all basic factors affecting a deformation of PVCT as a result of the processes running in the Setup are taken into account.

Below, we present the results of estimation of the energy release in two versions of changing the shape of a tube. It follows from them that the energy required for the appearance of observed deformations of PVCT ranges from 13 to 40 kJ.

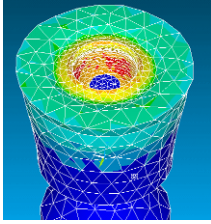
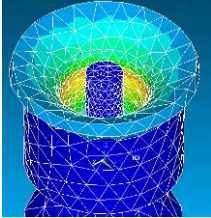
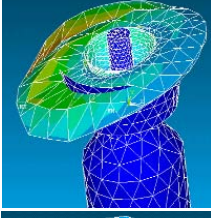
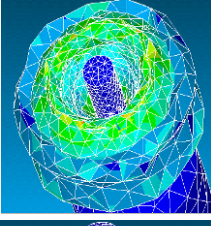
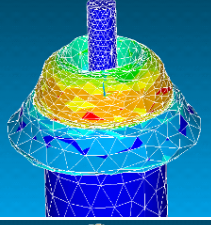
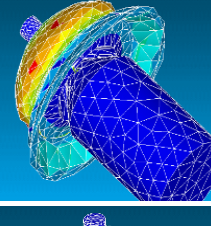
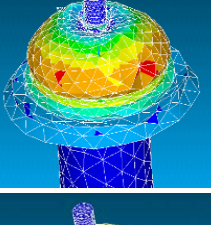
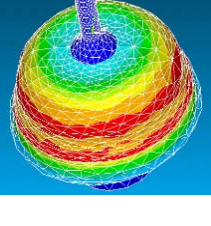
### **The results of modeling and the estimates of parameters of the action**

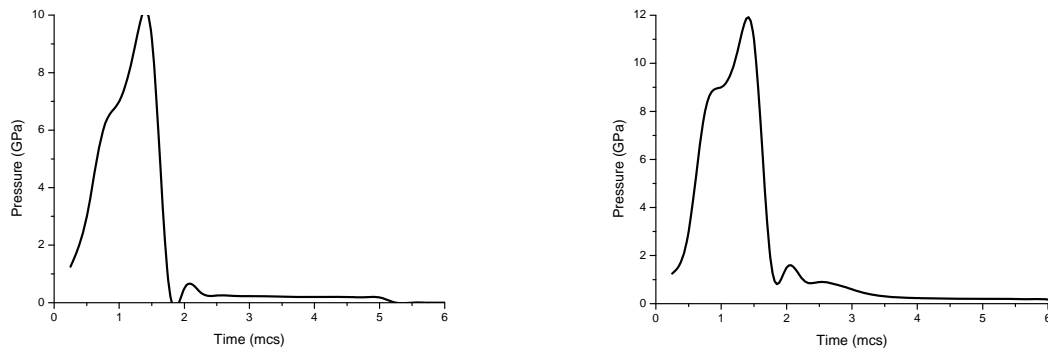
Let us consider two main experimentally observed versions of the deformation of PVCT: the full inversion without or with creeping on the rod positioned behind the tube. We denoted them, respectively, by B1 and B2. Figures 2 and 3 show the behavior of loads in B1 and B2 cases on the surfaces of PVCT subjected to the impact, for which the modeling results describe those observed in experiments.

It is worth noting that the solution of the inverse problem of determination of the characteristics of the action on PVCT indicates that the result is very sensitive to the values of parameters of the action and is valid for a quite narrow intervals of their magnitudes (Figs. 2 and 3).

In Table 2, we give the data of optical measurements of the characteristics of the flows of a substance that is the target – anode explosion products.

Table 1. Comparison of experimental and model final states of PVCT

	States of the tube in experiments	States of the tube by modeling	Comments
1			$E_{\text{def}}=5.8 \text{ kJ}$ , $E_{\text{kin}}=4.9 \text{ kJ}$ , <b>Total energy – 10.7 kJ</b>
2			$E_{\text{def}}=9.3 \text{ kJ}$ , $E_{\text{kin}}=7.1 \text{ kJ}$ , <b>Total energy – 16.4 kJ</b>
3			$E_{\text{def}}=9.8 \text{ kJ}$ , $E_{\text{kin}}=8.2 \text{ kJ}$ , <b>Total energy – 18 kJ</b>
4			$E_{\text{def}}=16.4 \text{ kJ}$ , $E_{\text{kin}}=15.6 \text{ kJ}$ , <b>Total energy – 32 kJ</b>
5			$E_{\text{def}}=18.5 \text{ kJ}$ , $E_{\text{kin}}=17 \text{ kJ}$ , <b>Total energy – 35.5 kJ</b>
6			$E_{\text{def}}=24 \text{ kJ}$ , $E_{\text{kin}}=18 \text{ kJ}$ , <b>Total energy – 42 kJ</b>
7			$E_{\text{def}}=24 \text{ kJ}$ , $E_{\text{kin}}=18 \text{ kJ}$ , <b>Total energy – 42 kJ</b>
8			$E_{\text{def}}=29 \text{ kJ}$ , $E_{\text{kin}}=26 \text{ kJ}$ , <b>Total energy – 54 kJ</b>



*Figs. 2 and 3. Pulse loads on PVCT for the full inversion (B1) and for the creeping on a rod (B2).*

*Table 2. Data of optical measurements of the flows of explosion products*

Chem Elem ent /A	Mean energy of an ion, keV	Mean speed of an ion, cm/sec	Energy yield, J	Number of nucleons	
					%
H	1.65E-01	1.78E+07	2.49E+02	9.51E+18	1.73
Zn/65	7.56E+00	1.49E+07	4.78E+02	2.58E+19	4.70
Ni/59	4.21E+00	1.18E+07	2.83E+01	2.47E+18	0.45
N/14	9.73E-01	1.16E+07	2.54E+01	2.29E+18	0.42
O/16	9.09E-01	1.05E+07	8.39E+01	9.23E+18	1.68
Si/28	1.46E+00	1.00E+07	2.35E+01	2.83E+18	0.52
Co/59	3.01E+00	9.94E+06	2.23E+01	2.73E+18	0.50
P/31	1.29E+00	8.96E+06	9.36E+00	1.41E+18	0.26
Ti/48	1.64E+00	8.13E+06	4.87E+01	8.90E+18	1.62
Al/27	8.23E-01	7.68E+06	4.94E+01	1.01E+19	1.84
Cu/64	1.91E+00	7.62E+06	8.77E+01	1.82E+19	3.31
Pb/207	5.20E+00	6.96E+06	9.63E+02	2.40E+20	43.6
V/51	1.17E+00	6.67E+06	3.72E+01	1.01E+19	1.84
Ca/40	8.92E-01	6.56E+06	1.75E+02	4.90E+19	8.90
C/12	2.62E-01	6.49E+06	3.92E+01	1.12E+19	2.04
Fe/56	1.18E+00	6.39E+06	4.29E+01	1.27E+19	2.31
Mn/55	1.09E+00	6.18E+06	1.82E+01	5.74E+18	1.04
Na/23	2.48E-01	4.57E+06	1.04E+01	6.03E+18	1.10
Cr/52	3.87E-01	3.79E+06	5.35E+00	4.49E+18	0.82
F/19	5.80E-02	2.43E+06	9.87E+00	2.02E+19	3.67
S/32	7.18E-02	2.08E+06	1.27E+01	3.54E+19	6.44
K/39	4.04E-02	1.41E+06	1.03E+01	6.20E+19	11.3
In all:			2.43E+03	5.50E+20	100

The results of optical diagnostics of the flows of explosion products are presented in Table 2 and allow us to construct the empiric curve of the pressure variation, by summing the momenta of ejected particles after the explosion of the target – anode, which are distinguished by speeds and masses. The curves (see Fig. 4) obtained by these data are similar to those given by the modeling with the pressure shown in Figs. 2 and 3.

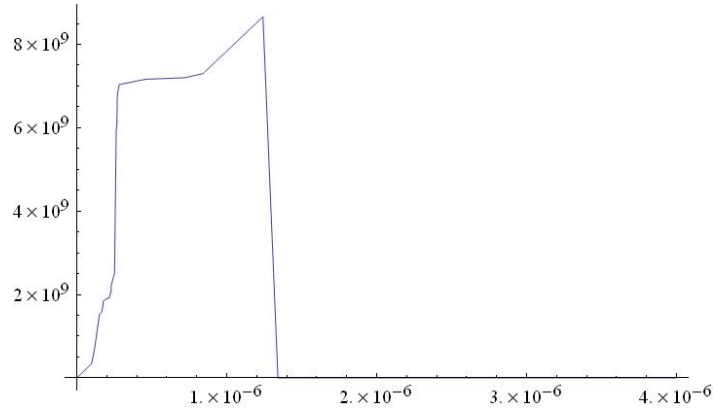


Fig. 4. Summary pressure of the substance flows acting on PVCT on the basis of empiric data

The differences of the curves are caused by a complicated character of the interaction of the flows of particles and plasma formations with the PVCT surface. For these plots, the common specific feature is the impact-wave character of a front formed by the flow of light elements and elements with medium atomic masses. Following these elements, heavy elements approach the surface of PVCT and form the maximum pressure. Since the last flows of heavy elements move near the surface of PVCT in the medium formed by the flows of elements arrived earlier, the pressure is damped, and the pressure on the tube surface decreases on the final stage. The total duration of the process is at most 2  $\mu\text{sec}$  by the data of Table 2 and by the modeling results.

We now explain the means of construction of the empiric curve of the pressure of explosion products (see Fig. 4). Each component of the flow transfers some momentum to PVCT during the corresponding time interval, by creating a pressure pulse. Such a component reflects from the surface of PVCT, is mixed with previously arrived components during several collisions, and is thermalized near this surface. This happens practically instantly at high densities of a gas-plasma cloud and its sufficiently low temperature.

The mean speed of particles in a plasma formation is low, and the dissipation of the energy and the density of particles in it are determined by thermal speeds on the boundary. The thermal speed is

determined by the formula  $v_0 = \frac{1.610^6 \sqrt{T}}{\sqrt{A}}$  [cm/sec] ( $A$  – mean atomic weight,  $T$  – plasma

temperature in eV) [5]. In the time  $t$  after the arrival of the last (slowest) flow component to PVCT (according to Table 2, this time is equal to 1.3  $\mu\text{sec}$ ), the components of flows can move from PVCT with the thermal speed  $v_0$  at the maximum distance of about  $R(t) = v_0 t$ . We approximate the corresponding region by a sphere with radius  $R$ , which contains about  $10^{20}$  atoms by the data of Table 2 [4], and estimate the pressure produced by such gas-plasma cloud on the PVCT surface.

The temperature of a near-surface plasma formation is rapidly established approximately at a level of 3 eV due to the practically instantaneous thermal emission at the high temperature  $\sim 10^8$  K and a high frequency of collisions and decreases down to 2.3 eV in the time 1.8  $\mu\text{sec}$ . This drop in the temperature occurs due to the energy transfer into the emission by the Stefan-Boltzmann law. Let us estimate the energy loss at the time  $t$  by a weakly ionized spherical cloud with radius  $R(t)$ . For the unit time, the emission intensity from the cloud surface is

$$\frac{dE}{dt} = 4\pi\sigma T^4 (v_0 t)^2.$$

The integration of this equation gives the time dependence of the energy of the plasma formation,

$$E(t) = E_0 - \frac{4}{3}\pi\sigma T^4 v_0^2 t^3, \quad (1)$$

where  $E_0$  is the energy transferred by the flow to the plasma cloud under its formation.

For the speed of the lead component with  $A=207$  (which is principal and taken as typical), we obtain  $v_0 \approx 2 \cdot 10^5$  cm/sec. In other words, the radius and the volume of the sphere vary from the initial values  $R_0 \sim 1$  cm and  $\sim 4$  cm<sup>3</sup>, which are determined by the geometry of PVCT, at the time moment 1.3 μsec to  $R \sim 1.3$  cm and  $\sim 7$  cm<sup>3</sup> at the time moment 1.8 μsec, respectively. In this case, the density of ions and atoms in the sphere varies from  $6.1 \cdot 10^{18}$  cm<sup>-3</sup> down to  $\sim 10^{18}$  cm<sup>-3</sup> [6].

We estimate the pressure on the tube surface from the side of a plasma cloud to be  $nkT$  for the whole time interval, when the cloud exists. With regard for the values of density and temperature of the gas-plasma cloud, its value  $\sim 0.7$  MPa, which is a small part of the total pressure on PVCT and is omitted in what follows.

In the course of modeling, we obtained the following data on the components and the parameters of the action on PVCT:

1. **Duration of the force action.** In order to deform PVCT in B1 and B2 cases, the force action for about 2 μsec was realized; then the deformation and the motion of the tube had the inertial character.
2. **Force action on PVCT.** The application of a pressure to the impact-subjected surfaces was started at the zero time moment at the initial value of about 10 MPa on the end of the tube and the amplitudes 9 GPa and 11.5 GPa for B1 and B2, respectively.
3. **Duration of the shape-forming processes.** The total duration of the full inversion of PVCT was approximately 10 μsec without its further motion and about 15 μsec in the case of the motion of PVCT along the cylindrical electrode.
4. **Total mechanical energy required for the observed deformations of PVCT.** The intervals of energies received by PVCT during the realization of B1 and B2 versions were 13÷22 kJ and 32÷54 kJ, respectively.

Having obtained a change of the shape of PVCT within the model, which agrees well with the deformation observed in experiments, we carry out the process of minimization of the energy received by PVCT. To this end, the initial configuration of loads was varied so that a decrease of the energy received by PVCT did not violate the type of deformation under consideration.

We note that both types of the modeling of a change of the form were realized in the elasticity approximation, at which no energy dissipation by means of its transformation into the thermal energy occurs. Thus, the tube energy acquired under the action includes only two components: deformational and kinetic ones. The kinetic energy of the tube is represented by the energy of motion of its parts irrespective of the motion of the center of masses. When a required variation of the form is attained, the tube shape, the deformational energy, and the kinetic energy of the tube oscillate around some mean values (they are taken below as the deformational and kinetic energies of the tube). The total mechanical energy does not vary after the termination of a force action on the tube. The real tubes in experiments on the Setup are heated, starting from a certain time moment, which leads probably to some physico-chemical transformations in the material of tubes. As a result, PVCT undergoes not only elastic, but also plastic changes on the final stage of a real deformation. After some number of oscillations, the kinetic energy of a real tube dissipates into the thermal energy, which dispersed in the course of time over the Setup, and some part of the mechanical energy is stored in the form of that of strains.

We have performed series of numerical experiments within the model of PVCT aimed at the study of a possibility of the inversion of a tube only under the action of Coulomb forces caused by the charge accumulated on the tube surface without consideration of the action of an impact load on the tube induced by the flows of target – anode explosion products. It was assumed that the currents (charges), which pass in the unit of the Setup including PVCT, cause the accumulation of charges on the internal surface of the tube in a sufficiently thin layer and, respectively, the appearance of the pressure forces stretching the tube. They would finally cause at least one kind of inversion.

We considered various versions of the location of charges on the internal surface of the tube, including a uniform distribution of charges along the symmetry axis of the tube and some inhomogeneous distributions of charges, which would be formed at the passage of the flow of

electrons. At a uniform distribution of charges, we considered the limiting pressure (of the order of 12 GPa close to the fracture threshold for polyvinyl chloride) caused by the Coulomb repulsion. The uniform pressure on the internal surface of the tube (limiting) did not cause such deformations of the tube, which would be interpreted as those close to the inversion. The tube was stretched along the radius and compressed in the direction of the axis.

It was shown that the distribution of a negative charge over the internal surface of the tube can realize a considerable extension of the tube normally to the axis of the system, which is comparable with or exceeds its initial size. However, a partial or full inversion, which is characteristic of the observed deformations of PVCT, does not occur for any model charge distribution over PVCT.

A similar auxiliary role is played by a charge supplied on the PVCT surface (for the scenario with inversion of the tube). This is clearly supported by the case where a two-layer tube was used in experiments. The external layer was inverted, whereas only the inner surface of the internal layer of PVCT can be charged.

### **Target – anode explosion energy**

In view of the energy released on PVCT, as an element of the construction of the Setup seen at a certain solid angle from the “hot dot,” by ejected target explosion products, we will find the lower bound for the energy released in the central region of a target.

On the initial stage, the dispersion of target – anode explosion products is spherically symmetric. According to the nature of the basic processes running in the diode on the initial stage of the explosion, the dispersed shell of products is a mildly ionized plasma subjected to the action of electrodynamic forces in the diode chamber. The composition of this plasma includes various components forming the flows strongly interacting with one another due to the collisional friction under high concentrations of particles in flows. On the initial stage, their density is high so that the medium formed by them is optically opaque. While the primary shell is spreading, these flows can be separated due to both a decrease of the density and a higher mobility of light elements, and the medium itself becomes transparent for quanta of light [7].

In a theoretical description, the medium composed by flows can be considered in the MHD approximation, in which the substance is described in terms of the mean speed and density. The external magnetic field, field of the electron component, collisional friction, pressure, and viscosity should be taken into account [4].

When the flows of a substance approach the surface of elements of the diode chamber, they render a time-dependent spatially distributed hydrodynamical pressure on them and, in particular, on PVCT. In this case, there arise the plasma formations, where the kinetic energy of flows is transformed into the internal energy on such a level that their thermal pressure on the initial stage is comparable with the primary hydrodynamical pressure. But then the former becomes less than the latter.

Therefore, we need to consider the following main aspects of the dispersion of explosion products:

1. Evolution of a dense gas-plasma shell after the explosion of a target – anode.
2. Anisotropy of the dispersion of explosion products in the volume of the diode chamber.

Accordingly, we introduce the following coefficients:

1.  $K_1$  - ratio of the total energy of the explosion to the optically observed energy ( $E_{\text{ex}} = K_1 E_0$ );
2.  $K_2$  - ratio of the energy released from the target to the energy supplied to PVCT.

We now consider the inverse problem of determination of the target explosion energy as a result of the analysis of the dispersion of explosion products with regard for the energy released on PVCT.

### Anisotropy of the dispersion of explosion products in the diode chamber (estimation of the coefficient $K_2$ )

Consider the stage preceding the pressure on the tube surface, during which the energy is supplied from the explosion region to the tube surface.

The results of solution of the system of partial differential equations describing the dynamics of fields and the motion of target – anode explosion products showed that, under conditions of the experiment, a certain part of trajectories falls into a given region of the diode chamber due to the magnetic field. The final time-dependent spatial pressure of target explosion products on units of the system is formed by the family of possible trajectories of the dispersed explosion products. We established the strong dependence of the calculated pressure evolution on a number of the following parameters:

- Amplitude and phase of the current or the magnetic field and the radius of a cylinder, where the electrical current passes;
- Contribution of the thermal or kinetic component to the gas-plasma pressure;
- Coefficient of collisions of neutral and charged explosion products;
- Mass composition and speeds of the explosion-produced flows of particles (these parameters are essential for the separation of components of the flows on the stage, where their density decreases).

Table 2 presents the data of optical measurements of the flows of target explosion products. In our calculations, we use the data on the composition of the flows of atoms and their speeds, as well as the relative percent energy characteristics of the flows.

The analysis of trajectories given in Fig. 5 implies that the time moment, when the characteristic flows (hydrogen and lead) approach the PVCT surface (whose axial section is shown by a rectangle in the left upper corner of Fig. 5), is determined by the speed of the relevant component.

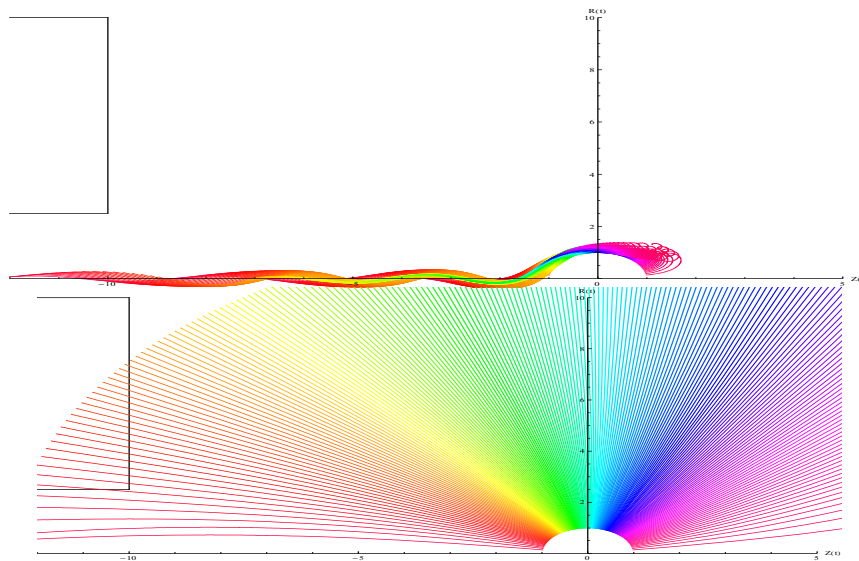


*Fig. 5. Hemisphere of the dispersion of explosion products (from top to bottom: hydrogen in 35 nsec and lead in 100 nsec after the explosion)*

It is seen that the lighter elements approach the tube surface along curved trajectories, whereas the heavy elements move along almost rectilinear paths. In this case, for a time interval of at most 2  $\mu$ sec, a hydrodynamic pressure pulse 9 GPa in amplitude due to heavy elements is formed on the end of the tube. As for the internal cavity of the tube, it contains practically all flows under consideration, which form the pressure pulse on its surface. Under conditions of the diode chamber where the electromagnetic fields are created, these two pressure pulses possess different spatial anisotropies. So we have impacts of the flows on the tube end and on the internal surface of the tube.

Figure 6 represents the phase plane of trajectories under the dispersion of explosion products. Blue, red, and green colors indicate trajectories starting, respectively, at the nearest, middle, and farthest points of the initial explosion sphere relative to PVCT.

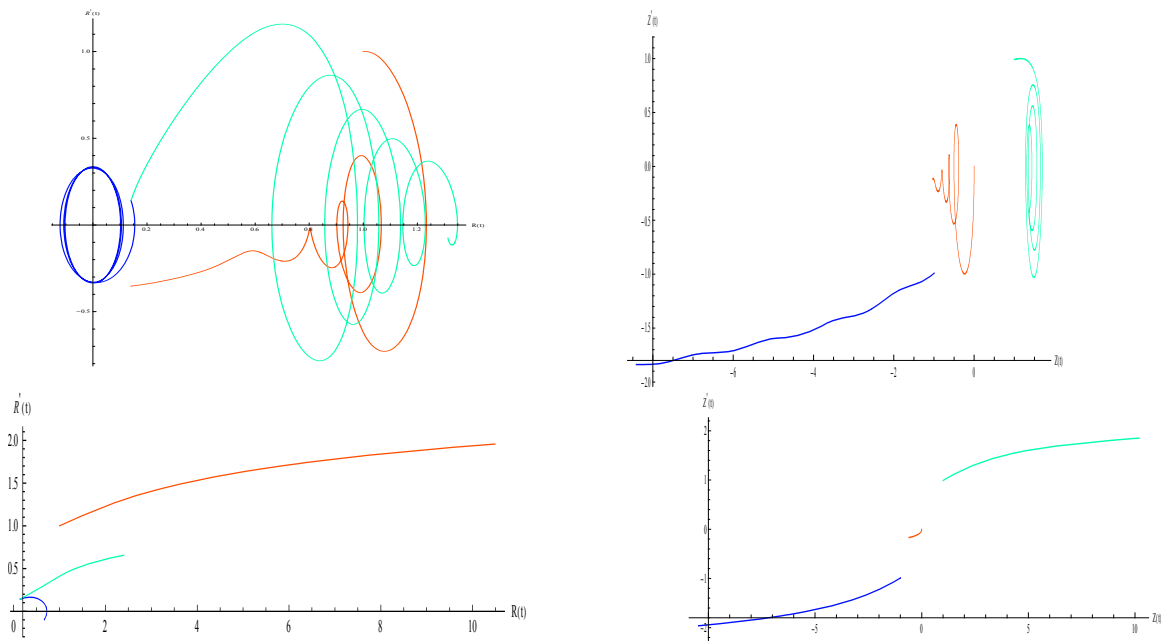


Fig. 6. Phase portraits demonstrating the anisotropy of ejected target – anode explosion products (from top to bottom: hydrogen and lead). To the left – phase plane  $R-R'$ , to the right – phase plane  $Z-Z'$ .

During the dispersion, only the flows of heavy elements presented by lead in Figs. 5 and 6 have almost isotropic character. Hence, the tube volume is filled by a part of these flows corresponding to the solid angle of the tube seen from the coordinate origin of the sphere formed by ejected products of the explosion for these figures.

The calculations showed that this solid angle is equal to approximately 1/8 of the total solid angle. Therefore, 7/8 of the flow of heavy elements do not fall in the region of the tube. We note that the flows of light elements can circumvent sometimes the tube. In these partial cases, the estimates of the explosion energy turn out, of course, understated.

For heavy elements by virtue of their almost isotropic dispersion in a wide range of conditions, the estimate of the loss of 7/8 of the total flow of heavy elements seems to be justified. Hence, the registration of the energy  $E$  on the tube means that, at the explosion, the flows of heavy elements received the energy equal to  $8E$ , from which  $7E$  “bypassed” PVCT.

According to the data of Table 2, the heavy elements cover  $\sim 2/3$  of the optically measured explosion energy. Hence, we obtain the coefficient  $K_2 = E/((1/8)2/3E + 1/3E) = 2.4$  for the calculation of the total energy received by the flows of particles ejected at the explosion by the energy supplied to the tube.

Thus, if the tube has received, according to the above-presented estimate, from 32 to 54 kJ, the total energy released at the explosion is from 80 до 130 kJ.

We now consider the distribution of the speeds of explosion products, which have received some initial energy and then change their trajectories with regard for the experimental conditions realized on the Setup. We will present the results of solution of the system of equations of motion of the flows with the characteristic values of initial dispersion speed  $V_0$  equal to  $3 \cdot 10^3$  and  $7.5 \cdot 10^4$  m/sec and of mass  $\sim 10^{-2}$  g, which was lost (by experimental data) by the target – anode as a result

of the explosion. In calculations and in plots, we use the system of measurement of distances in units of the target – anode thickness ( $l \sim 1$  mm), speeds in units of  $V_0$ , and the time in units of  $(l/V_0)$ .

Assuming that all mass lost at the explosion was ejected into the extending sphere with the velocity  $V_0 = 3 \cdot 10^3$  m/sec, we obtain the kinetic energy  $\sim 100$  J. This value is significantly less than the energy of flows ( $\sim 32$  kJ), which was released, according to our measurements, in the region of the cathodic PVC tube. By the trajectories in Figs. 7 and 8, it is seen that, first, the flows leave the explosion region slowly, and, second, their speeds equal to  $V_0$  at the initial time moment decrease and become far from values given in Table 2.

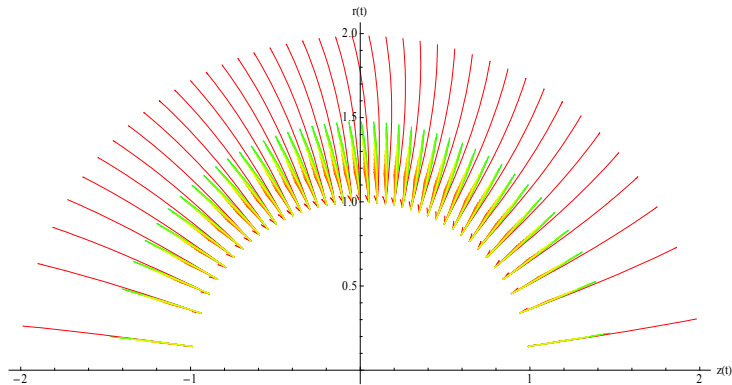


Fig. 7. Trajectories of the flows ejected from the explosion region at  $V_0 = 3 \cdot 10^3$  m/sec in coordinates  $(R,Z)$

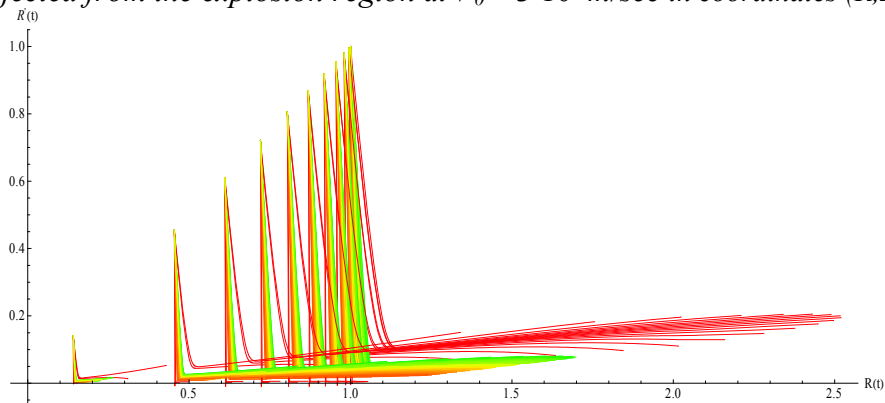


Fig. 8. Trajectories on the phase plane  $(R,R')$  at  $V_0 = 3 \cdot 10^3$  m/sec; the initial point of trajectories –  $(1,1)$

If we choose the initial speed  $V_0 = 0.75 \cdot 10^5$  m/sec, then the upper bound for the kinetic energy is 30 kJ, which is comparable with the minimum value of the energy of flows ( $\sim 32$  kJ) obtained above, while considering the deformation of the tube. By the trajectories in Figs. 9 and 10, it is seen that the flows started from the explosion region become strongly separated in the space and by their speeds. The speeds of some explosion products decrease below 1, whereas some speeds increase to 3-4 and, on this level, are comparable with values from Table 2.

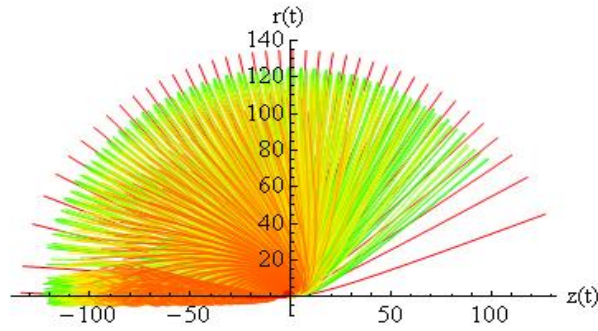


Fig. 9. Trajectories of flows on the plane  $(R,Z)$  at  $V_0 = 0.75 \cdot 10^5$  m/sec

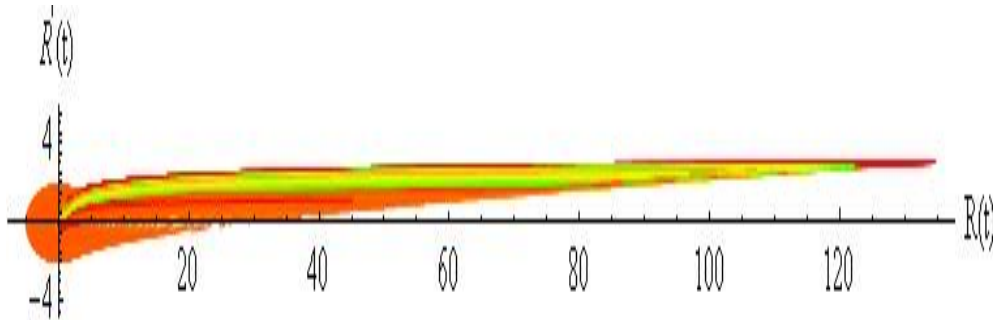


Fig. 10. Trajectories on the phase plane  $(R,R')$  at  $V_0 = 0.75 \cdot 10^5$  m/sec

Thus, the result obtained indicates the correspondence of the calculated distribution of speeds for the whole collection of the registered flows of particles (from hydrogen to lead) to the data of Table 2.

### Optical measurements of the dispersion of explosion products

By the data of Table 2, the energy of all ejected target – anode explosion products calculated with the use of the results of optical measurements is 2.4 kJ. At the same time, the previous calculations have substantiated that the energy released at the explosion of a target is of the order of 80 kJ, so that about 32 kJ falls in the solid angle of PVCT. We will try now to answer the question why only 2.4 kJ from 80 kJ released at the target explosion are registered.

The gas-plasma medium formed at the target – anode explosion is a dense ball (or a spherical layer), where the flows of elements are sufficiently mixed, and the emission of the energy from this spreading sphere can be considered in the approximation of absolutely black body. The calculations by formula (1) indicate that the energy emitted from the surface of this absolutely black body in the diode chamber is of the order of 2.4 kJ, if the temperature of this body is 1.2 eV, which is a quite realistic value in the case under consideration. We may state that the observed energy does not exceed significantly the emission energy of the object in the approximation of absolutely black body. Inside the surface of the exploded sphere as a black body, some (significant) part of the energy remains invisible in the optical measurements.

The point consists in that the elementwise data in Table 2 are related to the stage of the dispersion of explosion products, when the medium becomes optically transparent to some extent. This stage is preceded by the state of the exploded target – anode with much higher values of density and temperature of a substance, which is optically opaque.

We note that the key role for the medium transparency in optical measurements is played by the Rosseland mean free path of quanta of light in the medium:

$$l_p = \frac{10^{22} T^{7/2}}{z N^2} \begin{cases} 480 z^{-2} \\ 1.3 (z^2 + z)^{-1} \\ 4.4 (1 + z)^{-2} \end{cases}, \quad (2)$$

where  $T$  – plasma temperature in Kelvin degrees,  $z$  – ionization degree of an atom emitting a light quantum;  $N$  – density of ions in the medium, where quanta propagate; three terms after the brace correspond to different possibilities for light to be absorbed in the medium (free-free exchange by photons and one- and multiply ionized atoms) [7].

If the size of the medium exceeds the Rosseland mean free path for a quantum emitted by an atom, the quantum is absorbed by the medium, and the optical device does not register it. The main factors affecting the optical transparency under the dispersion of explosion products are the plasma temperature  $T$  and the density of ions in the medium. The density decreases, as the exploded sphere propagates. For the spreading sphere with radius  $r$ , the density can be approximately calculated by the formula

$$N = N_0 \frac{r_0^2}{r^2}.$$

The optical measurements in the experiments under study present the data on the process of dispersion from the start of the explosion till the time, when the sphere touches the walls of the diode chamber. In the course of this process, the density of ions decreases to a value determined by the spreading sphere with maximally possible radius. Let us assume that the thickness of the spreading spherical layer is equal to 0.1 cm, the radius of the initial “hot dot.” By calculating by formula (2) for the zero time moment of the existence of the spreading sphere, we obtain that the Rosseland mean free path is negligible as compared with the sphere radius. In other words, the optical emission is very low.

As the plasma spherical layer of explosion products extended, the density of ions in it decreases, and it becomes more and more transparent for quanta of light. The transparent layer is adjacent to the external spherical surface and has a thickness equal to the Rosseland mean free path  $l_p$ . In our case, the thickness of the whole layer  $d$  is not large, all the spherical surfaces have the close areas  $S$ , so that the volume of the spreading layer is equal approximately to  $dS$ , and the volume of its transparent part is  $l_p S$ . The ratio of the energy  $E_0$  stored in the transparent layer to the energy  $E_s$  of the whole spreading layer with approximately uniform energy distribution is equal to the ratio of the volumes of these layers:

$$E_0 / E_s \approx (l_p S) / (d S) \approx l_p / d. \quad (3)$$

In the case under consideration, the ratio of the energy measured optically to the explosion energy is  $E_0 / E_s \approx 1/40$ . Then formula (3) yields  $l_p \approx d/40$ .

Let the external radius of the sphere attain 15 cm (when it touches the walls of the chamber). Then the spherical layer of explosion products has a thickness of 0.1 cm, and the temperature of plasma in this layer is about 0.3 eV. For the medium density equal to  $10^{18}$  ion/cm<sup>3</sup>, the Rosseland mean free path turns out to be 0.0025 cm by formula (5), i.e., the spreading substance is visible at depths from the external surface of the sphere of at most 0.0025 cm. At the same time, the quanta from deeper points cannot be registered by optical lenses positioned on the periphery of the diode chamber.

By this mechanism, the essential share of the energy released at the explosion is not registered optically, though it induces the energy-consuming deformation of PVCT observed in experiments.

## Conclusions

We have estimated the minimum energy released at the target – anode explosion to be 80 kJ. It is known that the energy of the power supplies used in the experiment is about 60 kJ. Thus, even if we assume that the entire energy of the power supplies was delivered to the region occupied by a target, we obtain that the energy efficiency of the Setup is more than 1.

Moreover, the analysis of the results of measurements of the electrical currents in various parts of the Setup and the transport of the electromagnetic pulse allowed us to estimate the energy supplied directly to the target – anode as 0.6 kJ. Thus, the efficiency of the energy source driven in the anode of the hard-current diode by a beam of electrons as high as  $Q > 100$ .

The estimated energy released at the explosion equal to 80 kJ corresponds to the temperature of a substance of the exploded target – anode to be 7 keV or  $\sim 10^8$  K. To comment such a high temperature, we emphasize that such experimentally attained densities ( $10^{23} \div 10^{18}$  cm<sup>-3</sup>) and the relatively large time of the dispersion of a substance ( $10^{-7} \div 10^{-6}$  sec) allow one to carry out, for example, the (D,T) thermonuclear reaction in the macroscopic volume of a spreading target – anode by the scheme of stationary confinement of plasma.

It is impossible to obtain such high values of energy yield with the use of the traditional approaches to the inertial fusion of nuclei [11] and, all the more, with a copper target – anode due to low parameters of the flow of electrons from a primary driver. However, such energy release in a copper target – anode is possible under a realization of the collective nuclear fusion described in book [1] in detail. This book contains the experimental results obtained by the electrophysical methods, methods of mass-spectrometry, X-ray diffraction, etc., and their theoretical analysis and outlines some ways of the further studies.

## References

1. S.V. Adamenko, F. Selleri, A. van der Merwe, Controlled Nucleosynthesis. Breakthroughs in Experiment and Theory (Springer, Berlin, 2007).
2. O.C. Zienkiewicz, The Finite Element Method in Engineering Science (McGraw-Hill, London, 1971).
3. L.J. Segerlind, Applied Finite Element Analysis (Wiley, New York, 1984).
4. D.A. Frank-Kamenetskii, Plasma – the Fourth State of Matter (Plenum, New York, 1972).
5. S.I. Braginskii, Transfer Phenomena in Plasma, in: M.A. Leontovich (Ed.), Problems of Plasma Theory (Gosatomizdat, Moscow, 1963), Iss. 1, p. 183 (in Russian).
6. E.V. Shpol'skii, Atomic Physics (Iliffe, London, 1969).
7. A.F. Aleksandrov, A.A. Rukhadze, Hard-Current Electrodischarge Sources of Light, Usp. Fiz. Nauk, **112**, Iss. 2, 193-230 (1974).
8. V.A. Kabanov (Ed.), Encyclopedia of Polymers (Sov. Entsikl., Moscow, 1974), Vol. 2 (in Russian).
9. V.I. Azarov, A.V. Burov, A.V. Obolenskaya, Chemistry of Wood and Synthetic Polymers (LTA, St.-Petersburg, 1976) (in Russian).
10. G.M. Bartenev, S.Ya. Frenkel', Physics of Polymers (Khimiya, Leningrad, 1990) (in Russian).
11. J.J. Duderstadt, G.A. Moses, Inertial Confinement Fusion (Wiley, New York, 1982).